^{13}C CPMAS NMR of Bright and Burley Tobaccos

Jan B. Wooten*

Philip Morris Research Center, P.O. Box 26583, Richmond, Virginia 23261-6583

^{13}C CPMAS NMR spectra were obtained of the leaf laminae and stems of cured bright and burley tobaccos. The solid phase NMR spectra of some of the most abundant tobacco components were also obtained, including cellulose, hemicellulose, and pectin (each isolated from tobacco), calcium and potassium salts of malic and citric acid, calcium oxalate, rutin, chlorogenic acid, and nicotine (in the form of a crystalline ditartrate salt). The tobacco spectra have been interpreted in light of these reference materials, as well as the chemical analyses of similar samples. Multiple cross-polarization contact times, interrupted decoupling, and single-pulse excitation were employed to improve the discrimination between overlapping resonances, to reveal new spectral features, and to detect tobacco components obscured by the complexity of the spectra. These alternative pulse experiments permitted the selective detection of microscopic calcium oxalate crystals, solanesol and other mobile waxes, nicotine, citrate, and fructose.

Keywords: *Bright tobacco; burley tobacco; plants; ^{13}C CPMAS NMR*

INTRODUCTION

The conventional approach to the total analysis of plant tissue relies on a tedious fractionation procedure, followed by wet chemical analysis of the separated components (Bokelman et al., 1983). Utilizing this strategy, Bokelman and Ryan analyzed bright and burley tobacco laminae and stems for the principal cell wall biopolymers (i.e. cellulose, hemicellulose, pectin, protein, lignin, and starch), as well as the most abundant low molecular weight components such as organic acids, sugars, and minerals (Bokelman and Ryan, 1985; Ryan et al., 1985). An elaborate analysis of this kind represents a substantial effort that is not practical for routine investigations. ^{13}C CPMAS NMR spectroscopy, which in recent years has been widely employed to characterize natural and synthetic solid materials, is a nondestructive method of analysis that can be a useful alternative to the wet chemical methods.

A variety of plant materials of commercial, agricultural, and botanical importance have been analyzed by ^{13}C CPMAS NMR. These include wood (Kolodziejski et al., 1982; Haw et al., 1984; Haw, 1989), grasses (Himmelsbach et al., 1983), forages (Cyr et al., 1990; Elofson et al., 1984), seeds (O'Donnell et al., 1981; Haw and Maciel, 1983), various herbaceous plants (Maciel et al., 1995), bean sprouts (Jarvis, 1990), celery strands (Jarvis and Apperly, 1990), apple (Irwin et al., 1984), oat and cotton seed hulls (Garleb et al., 1990), and cotton stalks (Yosef et al., 1994). Although a total plant tissue analysis is not possible by NMR, NMR does offer the advantage that many components, including the difficult to isolate high molecular weight biopolymers, can be observed without the need for chemical separation. Beyond this level of analysis, NMR can be combined with a simplified fractionation scheme to characterize the insoluble residues remaining after successive extractions of the plant tissue. This approach has been used, for example, for the analysis of wood (Kolodziejski et al., 1982) and for cell walls from *Vigna radiata* hypocotyls (Jarvis, 1990). Another alternative, which can be applied in some favorable cases, is the ^{13}C enrichment of specific molecular sites which can then be detected above the resonance background (Lewis et al., 1987).

The primary obstacle to a more complete analysis by NMR is the lack of sufficient spectral resolution to discriminate between all of the components. The carbon resonance lines of solid materials are typically much broader than they are for solutions. Consequently, if the chemical shifts of different components are similar, as they are for the various plant polysaccharides, there is usually significant overlap between their carbon resonances. In general, the resolution is not improved very much by obtaining the spectra at higher magnetic field, a strategy often used for solutions, because the resonance line widths typically increase in proportion to the applied field strength. There are, however, other experimental approaches that can help to improve the discrimination between some components or to reveal components or spectral features that are obscured by spectral overlap. These techniques include variable contact time and dipolar dephasing experiments, and the use of single radio frequency pulses instead of cross-polarization for observing the carbon nuclei.

In this paper, the ^{13}C CPMAS and single-pulse MAS NMR spectra of bright and burley tobacco laminae and stems are presented. The carbon resonances of the various polysaccharides and protein are identified, as are a number of low molecular weight components. The interpretation of the spectra is, for the most part, straightforward due to the availability of the chemical analyses of similar samples published by Bokelman and Ryan (1985). The tobacco spectra can be compared with the NMR spectra of other types of plants that have been previously reported and provide impetus for the further use of NMR for the characterization of plant materials.

MATERIALS AND METHODS

Experimental Samples. The tobacco samples employed were commercial, aged, uncased, and cured bright and burley tobacco laminae and stems. The samples were crumbled to facilitate spinning, but otherwise no additional preparation or treatment was made. Rutin, chlorogenic acid, and other organic acid salts were obtained from Aldrich Chemical Co. Nicotine ditartrate dihydrate was provided by Dr. John Paine.

* Telephone (804) 274-3465; fax (804) 274-2160; e-mail wooten@talos.pm.com.

0021-8561/95/1443-2858$09.00/0

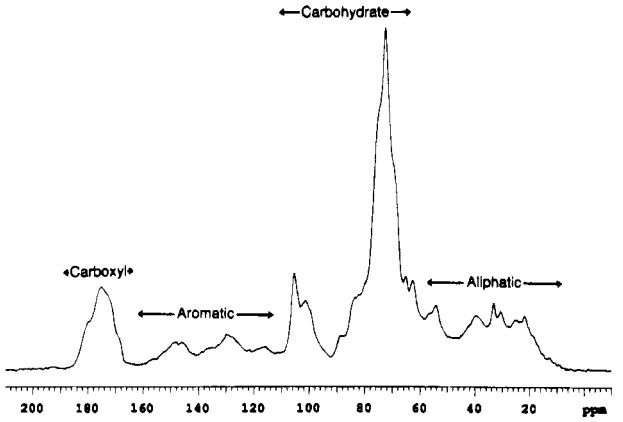

Figure 1. Typical ^{13}C CPMAS NMR spectrum of bright tobacco obtained with a 750 μs contact time showing the different spectral regions. The spectrum was processed with a simple Gaussian apodization function to improve the signal to noise ratio.

Tobacco pectin, hemicellulose, and cellulose were previously isolated (Bokelman et al., 1993) and provided by Mr. Bill Ryan.

NMR Spectroscopy. The ^{13}C MAS NMR spectra were obtained on a Varian Unity 200 spectrometer at carbon resonance frequency of 50.3 MHz. The NMR probe was a Doty Scientific high-speed magic angle spinning probe. For the cross-polarization experiments, the initial proton $\pi/2$ pulse was 6 μs, corresponding to a radio frequency field of 41.6 kHz. The Hartmann–Hahn match was made at this field strength, whereas the proton decoupling field during the acquisition was ca. 60 kHz. The acquisition time was 50 ms with a spectral width of 20 kHz. The pulse repetition time was 2 s for both the single-pulse and cross-polarization experiments. In the dipolar dephasing experiments, a 40 μs decoupler delay was employed. The sample cells were 7 mm cylindrical silicon nitride rotors with kel-F endcaps. Typically, the samples were spun at ca. 4 kHz; higher spinning speeds were avoided to minimize the migration of waxes and natural oils in the samples. The chemical shifts are reported relative to tetramethylsilane but were measured relative to the methyl resonance of hexamethylbenzene (17.36 ppm) in a separately obtained spectrum. Usually, signal acquisition was made over a period of 13–15 h to obtain a good signal to noise ratio for the weakest resonances. For the multiple contact time experiments used to measure T_{CH} and ^{1}H $T_{1\rho}$, 18 contact times ranging from 15 to 14 000 μs were employed for a total acquisition time of 48 h. Regression analysis was based on peak intensities using Varian software.

RESULTS

Spectral Assignments. A typical ^{13}C CPMAS NMR spectrum of a bright tobacco sample obtained with a 750 μs contact time is shown in Figure 1. The ^{13}C NMR spectra of tobacco exhibit the characteristic spectral features found in the spectra of other plant materials. The spectrum can be conveniently divided into four regions: the aliphatic region, 10–60 ppm; the carbohydrate region, 60–110 ppm; the aromatic region, 110–165 ppm; and the carboxyl region, 165–190 ppm. The aliphatic region contains carbon resonances due to the aliphatic carbons in protein, amino acids, organic acids, lipids, alkaloids, natural products and oils, etc. It also contains the methyl carbon resonances of acetyl side chains in hemicellulose and of sugars such as rhamnose. The carbohydrate region predominantly exhibits resonances of carbons bonded to oxygen. The polysaccharides (cellulose, hemicellulose, starch, and pectin) are the major components in this category. Monosaccharides (principally glucose and fructose), alkaloids (principally nicotine), and organic acids (principally citric and malic acid) also have resonances in this region. The aromatic region contains resonances due to protein and amino acid side chains, alkaloids, and phenolics such as lignin, chlorogenic acid, and rutin. The carboxyl region is comprised of the resonances of carboxyl and carbonyl carbons found in pectin, organic acids, amino acids, protein backbone carbonyls and side chain carboxyl groups, lignin, chlorogenic acid, rutin, etc. The protein peptide carbonyls, and the carboxyl carbons of pectin and organic acids, however, dominate this region.

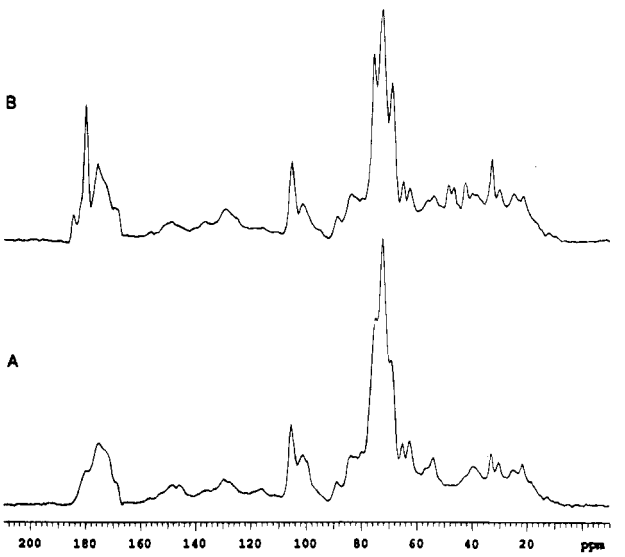

Figure 2. ^{13}C CPMAS NMR spectra of cured bright (A) and burley (B) tobacco laminae obtained with a 750 μs contact time. The spectra were processed with a shifted Gaussian apodization function to improve the resolution. The vertical scale of each spectrum is adjusted so that the intensity of the anomeric carbon resonance of cellulose at 105 ppm is the same in both spectra.

The ^{13}C CPMAS NMR spectra of cured bright and burley tobacco laminae are compared in Figure 2. To alleviate the spectral crowding of the overlapping resonances, the time domain signal (the FID) was apodized with a shifted Gaussian function before Fourier transformation to improve the spectral resolution. This procedure does not usually reveal features that are not evident in an unprocessed spectrum, but it does visually enhance some of the weaker features so that they are more easily distinguishable. The remaining spectra presented in this paper have been processed with this type of resolution enhancement, except as noted. The overall features of the bright and burley tobacco laminae spectra are similar, differing primarily in the relative intensities of their corresponding peaks. The resonance assignments can be made and their intensities interpreted in light of the analyses reported by Bokelman and Ryan (1985). The quantities of laminae and stem components quoted in this paper (in terms of percent of dry sample weight) are taken from their paper. Since the cellulose content of bright and burley tobacco laminae is nearly the same (5.9 vs 6.4% by weight, respectively), the vertical scale of each plot in Figure 2 has been adjusted so that the resonances of the cellulose anomeric carbon (C-1) at 105.3 ppm in each spectrum are equal in height. This allows comparisons to be made among the spectra relative to the amount of cellulose in each sample.

It is important to keep in mind that the resonance intensities in ^{13}C CPMAS NMR are affected by the efficiency of cross-polarization at each individual carbon site. In the cross-polarization experiment, proton spin

Table 1. ^{13}C Chemical Shifts (Parts per Million) of Solid, Polycrystalline Carboxylic Acid Salts Found in Tobacco

	methylene	hydroxymethine	carboxyl
monopotassium citrate	46.3, 47.0	74.4	178.5, 181.5
tripotassium citrate monohydrate	51.8, 53.8	77.1	178.2, 182.2
calcium citrate	45.2, 46.3, 49.0, 50.5, 51.8	74.5, 75.7	179.8, 183.1, 185.6
potassium malate	44.3	70.7	178.6, 182.0
calcium acid malate	42.2	69.0	179.8, 182.1
calcium malate	40.1	69.3	177.4, 181.1
calcium oxalate			167.6, 168.3, 169.2

polarization is transferred to the carbon spin system to gain an enhancement of the ^{13}C resonances. The duration of the transfer is called the contact time. At short contact times, the ^{13}C polarization grows with a characteristic time constant called the cross-polarization transfer time (T_{CH}). At longer contact times, the ^{13}C polarization decays due to the effect of proton rotating frame relaxation, described by ^{1}H $T_{1\rho}$. The contact time is usually chosen to achieve as uniform an enhancement as possible of the majority of resonances, so that quantitative comparisons can be made. By systematically varying the contact time, the 750 μs contact time employed for the spectra in Figure 2 was experimentally determined to be optimum for most of the tobacco resonances. Still, differences in the rates of cross-polarization for different types of carbons mean that there is an uncertainty in the absolute resonance intensity of individual resonances. Relative comparisons, however, should be more accurate. Some carbon resonances, however, do not reach optimum polarization near 750 μs and are thus underrepresented in Figure 2. These exceptions are noted below. Further issues related to quantitative measurements are considered under Discussion.

Aliphatic Region. From Figure 2, it can be seen that the overall intensity of the aliphatic region in the burley tobacco spectrum is greater than in the bright tobacco spectrum. This result mostly reflects the higher protein content of burley (10.4%) as compared to bright (6.8%) tobacco laminae. The relatively sharp resonance at 33 ppm in both spectra corresponds to carbons in polymethylene chains such as those found in hydrocarbon and fatty acid wax. The composite peak in the region between 45 and 50 ppm in the burley tobacco spectrum is essentially absent in the bright tobacco spectrum, although these resonances probably contribute to its resonance background. The center of the α-carbon resonances of protein falls in this region at ca. 48.8 ppm. The methylene carbon resonances of the various calcium and potassium salts of citric acid also fall between 45 and 54 ppm (see Table 1), but relatively few other resonances appear within this same region. Burley tobacco lamina is high in citrate compared to bright tobacco lamina (5.3 vs 0.7%, respectively). Thus, the peaks at 47 and 48 ppm in the burley tobacco spectrum must be due principally to protein α-carbons and citrate methylene carbons. The methoxyl carbon resonance at 54 ppm in both spectra is due principally to the methyl esterified carboxyl groups of pectin. Lignin contains numerous aromatic methoxyl groups, but the lignin content of both varieties of tobacco is only ca. 2%. Nicotine pyrollidine ring carbons exhibit resonances in the aliphatic region ranging from 21 to 41 ppm (Table 2), as can be seen from the spectrum of solid *l*-nicotine ditartrate shown in Figure 3A. However, no individual nicotine resonances can be definitively distinguished from the background in either the bright or burley tobacco spectrum, even though the nicotine content of tobacco is typically ca. 2–3% (Wynder and Hoffmann, 1967). This result should not be surprising since the line widths of the carbon resonances of the *in situ* nicotine can be expected to be broader than those shown in Figure 3A, due to a larger dispersion of chemical shifts resulting from the multitude of different conformations and intermolecular interactions in the tobacco lamina. It does appear, however, that the nicotine *N*-methyl resonance can be detected with the aid of a dipolar dephasing experiment (see below).

Carbohydrate Region. The carbohydrate region of the tobacco lamina spectra is dominated by polysaccharide carbon resonances. Low molecular weight sugars, rutin, chlorogenic acid, and other organic acids containing hydroxyl groups also exhibit resonances in the same region, but they mostly contribute to the resonance background (see Figure 3 and Tables 1 and 2). The profile of resonances in the carbohydrate region can be viewed as a composite of the spectra of the individual polysaccharide components. An examination of the ^{13}C NMR spectra of polysaccharides isolated from tobacco can aid in the assignment of the carbon resonances in the carbohydrate region of the intact lamina. The ^{13}C CPMAS NMR spectra of cellulose, hemicellulose, and pectin isolated from bright tobacco according to the Bokelman procedure are shown in Figure 4. The spectrum of starch is not shown, but it is expected to be very similar to that of hemicellulose. It can be seen from Figure 4A that the cellulose resonance lines are somewhat sharper than the resonances of either pectin or hemicellulose. The reason is that the polysaccharide chains in cellulose are organized into ordered microfibrils, whereas the pectin and hemicellulose polymers form random chains. The microfibrils provide a relatively uniform magnetic shielding for each type of carbon in the cellulose glycosyl units. This results in a smaller distribution of chemical shifts for each resonance than is typically observed in the spectra of the random chain polysaccharides. It is a general feature of ^{13}C CPMAS NMR of solids that ordered phases yield more narrow resonance lines than disordered ones.

Unlike the other tobacco polysaccharides, the cellulose spectrum exhibits two resonances for C-4 and C-6 of the glycosyl units. The ^{13}C spectra of cellulose samples taken from different plant and bacterial sources have shown that the individual carbon resonances of cellulose can exhibit significant differences in their line widths, intensities, and multiplicities, depending on the species of origin. These spectral variations are due to differences in the crystallinity and organization of the microfibril structure of the cellulose polymer (Vanderhart and Atalla, 1984). It is now well established that the resonances at 89.1 and 65.5 ppm can be attributed to C-4 and C-6, respectively, in the crystalline regions of the microfibrils. The intensity of these resonances relative to that of the corresponding resonances of the disordered regions appearing at 84.7 and 63.0 ppm, respectively, is a measure of the degree of crystallinity of the cellulose. By comparison of the tobacco cellulose spectrum to spectra of cellulose from other sources, it can be concluded that tobacco cellulose is somewhat less crystalline than cellulose typically found in hard or soft

Table 2. Chemical Shifts (Parts per Million) and Partial Assignments[a] for the Tobacco Natural Products in Figure 3

nicotine[b]	21.8 (C-4′), 26.4 (C-4′), 32.8 (C-3′), 38.7 (*m*), 41.4 (*m*), 54.4 (C-5′), [55.6, 60.3][c] (C-5′), 64.1 (C-2′), [68.6, 70.2][c] (C-2′), 125.1 (C-5), 126.6 (C-5), 133.1 (*n*, C-2), 145.4, 147.1, 148.3, 151.0
rutin	20.0 (*m*), 65.0, 70.0, 70.8, 71.8, 74.4, 77.4, 80.9, 97.1, 99.5, 103.5 (*q*), 105.3, 113.0, 115.5, 120.2 (*n*), 122.0, 136.0 (*n*), 143.1 (*n*), 148.0 (*n*), 154.3 (*n*), 155.5 (*n*), 160.1 (*n*), 162.5 (*n*), 176.9 (ester carbonyl)
chlorogenic acid	34.4, 36.1, 39.2, 69.6, 71.3, 73.1, 74.2, 76.9 (*q*), 112.8, 117.6, 125.9, 127.2 (*n*), 129.1 (*n*), 144.3 (*n*), 146.2 (*n*), 147.4 (*n*), 167.9 (ester carbonyl), 177.1 (carboxyl)

[a] *m* indicates methyl carbons, *q* indicates quaternary carbons, and *n* indicates nonprotonated aromatic carbon (identified by dipolar dephasing experiments). [b] The assignments given here are based on the published solution chemical shifts (Pitner et al., 1978; Slaven, 1984). This does not preclude the possibility that the order of some of the shifts may be reversed in the solid state. [c] ^{14}N quadrupole split resonance.

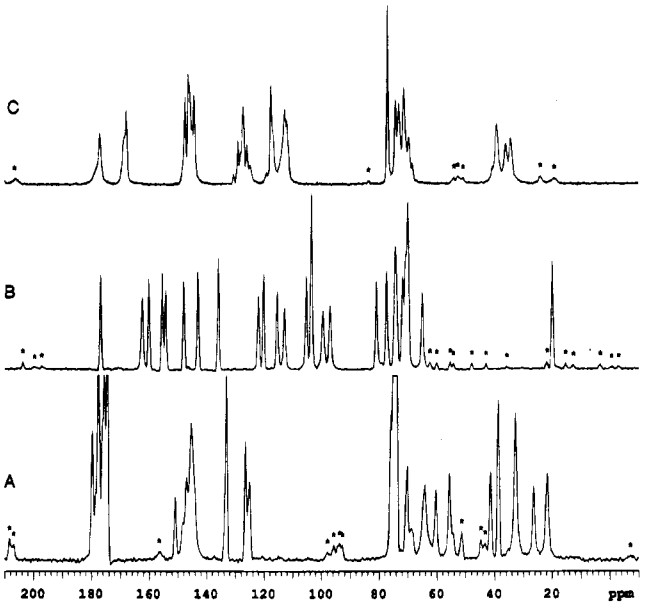

Figure 3. ^{13}C CPMAS NMR spectra of three abundant tobacco natural products: (A) *l*-nicotine ditartrate dihydrate, (B) rutin, (C) chlorogenic acid (predominantly *trans*). The off-scale peaks in the nicotine spectrum correspond to the tartrate moiety. Spinning side bands are indicated by asterisks.

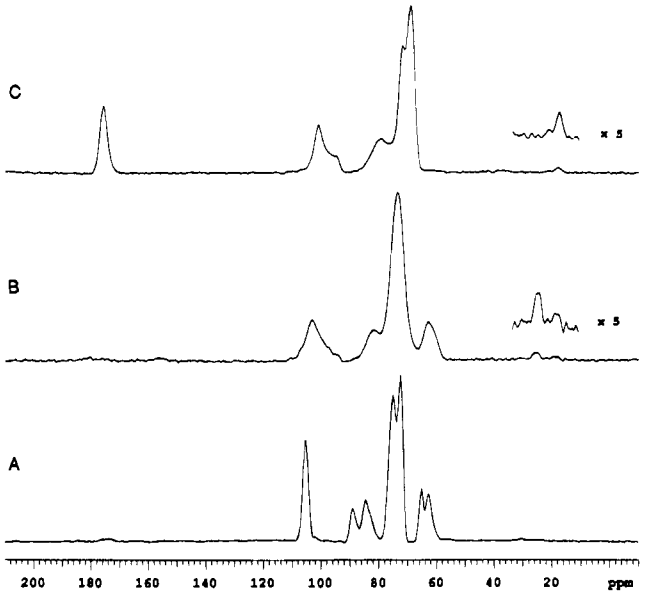

Figure 4. ^{13}C CPMAS NMR spectra of the most common tobacco polysaccharides isolated from bright tobacco: (A) cellulose, (B) hemicellulose, and (C) pectin.

woods (Newman and Hemmingson, 1990) and much less crystalline than cotton cellulose (Vanderhart and Atalla, 1984). The very harsh treatment required to isolate the tobacco cellulose from the other cell wall components, however, may have reduced its native crystallinity to some extent.

The pectic polysaccharide in bright tobacco consists of (1→4)-linked α-D-galacturonosyl residues interspersed with (1→2)-linked α-L-rhamnopyranosyl residues, which comprise ca. 4–5% of the total glycosyl residues (Sun et al., 1987). The predominant type of soluble hemicellulose appears to be arabinogalactan (Bokelman and Ryan, 1985). The resonance assignments of the pectin and hemicellulose carbons can be made by analogy to cellulose. The anomeric carbon (C-1) resonances appear farthest downfield in the range of 92–100 ppm due to the effect of bonding to two oxygen atoms. The anomeric carbon resonances of pectin and hemicellulose appear at 101.2 and 103.3 ppm, respectively. The remaining pyranose ring carbon resonances (C-2,3,4,5) appear at ca. 65–85 ppm; the peak maxima are 69.3 and 72.1 ppm for pectin and 73.8 ppm for hemicellulose. A single resonance appears at 63.0 ppm for the hemicellulose hydroxymethyl resonance (C-6). This resonance is absent in the pectin spectrum, since the C-6 sites in the galactoronsyl residues are either carboxylate or methyl ester carbonyl carbons. These resonances appear in the carboxyl region at 176 and 171.3 ppm, respectively. In the example shown in Figure 4C, the methoxyl carbon resonance of pectin does not appear, because the ester groups were hydrolyzed during the isolation procedure. For samples isolated under milder conditions, the methoxyl resonance appears at 54 ppm. By comparison of the integral of the methoxyl carbon resonance to the anomeric carbon resonance for such a sample, it was found that approximately 22% of the carboxyl groups in bright tobacco pectin are esterified, a result that agrees with previous solution NMR results (Westerlund et al., 1990). However, the degree of esterification determined from the CPMAS spectrum may be underestimated, due to the difference in cross-polarization efficiency between the anomeric and methoxyl carbon resonances (Irwin et al., 1985).

Other notable, weak features appear in the spectra of both pectin and hemicellulose. In the case of the tobacco pectin, upfield shoulders appear on the anomeric carbon resonance at 101 ppm, indicating that this polysaccharide has a nonuniform structure. The irregularities in the pectin structure can be attributed to the rhamnosyl residues in the galacturonan chain, as well as minor amounts of other neutral sugars such as arabinose, xylose, galactose, and glucose, which form side chain branches bonded to the rhamnosyl residues. The weak resonance at 18.3 ppm is due to the methyl carbon resonance of rhamnose (Irwin, 1989; Sun et al., 1987). The spectrum of tobacco hemicellulose in Figure 4B also exhibits upfield shoulders on its anomeric carbon resonance. Rhamnose is a minor component in the arabinogalactan polymer, accounting for as much as 14–17% of the neutral sugar residues. Lesser amounts of xylose, mannose, and glucose also occur (Bokelman and Ryan, 1985). The weak resonance at 25 ppm can be attributed to the methyl carbons of

acetylated glycosyl residues, and the very weak resonance at 18.4 ppm to rhamnose. The 18 and 25 ppm resonances can sometimes be observed in the spectra of intact tobacco laminae and stems, particularly if the samples have been water washed to remove some of the resonance background from soluble components.

Even though there is considerable overlap among the resonances of cellulose, pectin, and hemicellulose in the tobacco lamina spectra, some of the spectral features of the individual components can be distinguished. The spectra of the isolated polysaccharides in Figure 4 show that the overlap of the cellulose C-4 resonance at 89 ppm, or its anomeric C-1 carbon resonance at 105 ppm, with the resonances of either pectin and hemicellulose is comparatively small. Thus, these spectral features are easily distinguished in both the bright and burley tobacco spectra and can be used as a convenient basis for quantitative comparisons between tobacco types. It is also evident that the pectin resonance at 69 ppm appears farther upfield than any of the pyranose ring carbon resonances of either cellulose or hemicellulose. In the tobacco spectra, this resonance stands out as a prominent shoulder on the composite ring carbon resonance centered at 72.5 ppm. Unfortunately, there are no hemicellulose resonances that are easy to distinguish in the tobacco spectra, because they are broad and overlap with resonances of both cellulose and pectin, adding to the background of resonances without exhibiting any distinguishing features. The peak maximum of the hemicellulose anomeric carbon resonance does, however, appear slightly downfield (103 ppm) from the pectin resonance (101 ppm), providing some minimal discrimination.

Aromatic Region. The resonance peaks in the aromatic region are broad and nearly featureless. Specific spectral assignments are not very meaningful to make, but overall the aromatic carbon resonances can be attributed to alkaloids, aromatic amino acid and protein side chains, and phenolics, such as chlorogenic acid, rutin, and lignin. Nicotine contributes spectral intensity across the aromatic region, as can be seen from the ^{13}C CPMAS NMR spectrum of solid nicotine ditartrate shown in Figure 3A, but no individual resonances stand out. There are, however, some distinct differences between the bright and burley tobacco spectra in this region. Processing each spectrum to improve its signal to noise ratio, rather than the resolution, and plotting the spectra at a higher vertical scale allow the differences to be discerned more easily. The aromatic regions of the tobacco lamina spectra are shown in Figure 5. The vertical scale in each spectrum has been adjusted so that the anomeric carbon resonance of cellulose at 105 ppm has the same intensity. The ^{13}C NMR spectra of proteins in the solid state exhibit predominantly a single, broad resonance at ca. 130 ppm in the aromatic region (Baianu, 1989). Protein aromatic carbons thus account for a significant part of the resonance intensity at 130 ppm in the tobacco spectra. This explains the enhanced intensity of this resonance in the burley tobacco spectrum, since burley tobacco contains more protein. The bright tobacco spectrum exhibits resonances at 116.4 and 146 ppm that are more intense relative to the peak at 130 ppm than in the burley tobacco spectrum. Bright tobacco lamina is reported to contain ca. 0.7% rutin and ca. 1.5% chlorogenic acid, both of which have carbon resonances in the aromatic region, as shown in Figure 3B,C, respectively, and summarized in Table 2. In contrast, rutin and chlorogenic acid are nearly absent in burley tobacco lamina. The enhanced resonance intensity at 116.4 ppm in the bright tobacco spectrum relative to the burley tobacco spectrum is probably due to the contribution of chlorogenic acid.

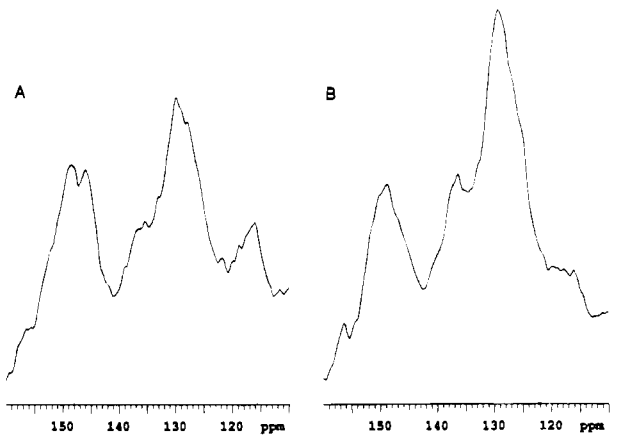

Figure 5. Expansion of the aromatic region of the ^{13}C CPMAS NMR spectra obtained with a 750 μs contact time of bright (A) and burley (B) tobacco laminae. The spectra were processed with a simple Gaussian function to improve the signal to noise ratio. The vertical scale of each spectrum was adjusted relative to the anomeric carbon resonance of cellulose.

Carboxyl Region. Carboxyl carbons in general cross-polarize more slowly than most of the other tobacco resonances because they lack a directly bonded proton. However, their cross-polarization rates are very similar in bright and burley tobacco (see Discussion). Thus, even though the overall intensity of the carboxyl region may be underrepresented in the respective spectra, comparisons between the spectra are still valid. The carboxyl region shows distinct differences between bright and burley tobacco laminae. The resonances at 184.7 and 180.0 ppm, which appear prominently in the burley tobacco lamina spectrum in Figure 2B, are much weaker in the bright tobacco spectrum in Figure 2A. These sharp low-field peaks can be attributed to potassium salts of organic acids, principally citric acid (see Table 1). Burley tobacco is reported to contain ca. 5.3% citric acid compared to only 0.7% in bright tobacco, whereas the amounts of malic acid are comparable (4.8 vs 3.7%, respectively). In addition, burley tobacco contains more aspartate, which exhibits a low-field amide carbonyl resonance at ca. 180 ppm (Wuthrich, 1976). The overall resonance intensity in the region 170–179 ppm and the intensity of the peak at 168.3 ppm are also greatest in the burley tobacco spectrum. The resonance intensity at 175 ppm results partly from protein peptide bond carbonyls. As the protein content of burley tobacco lamina is higher than in bright tobacco lamina, this resonance is correspondingly more intense. The resonance at 168.3 ppm is an interesting spectral feature that can be attributed to the carboxyl carbons of calcium oxalate. It exhibits unusual cross-polarization behavior and, with appropriate spectral processing, a multiplet splitting. Calcium oxalate is discussed below in detail.

Nicotine. The spectrum of solid polycrystalline *l*-nicotine ditartrate dihydrate in Figure 3A exhibits some unusual features that warrant further comment. A number of the resonances appear as pairs of peaks. While this doubling can be explained by the presence of two nonequivalent conformations of nicotine in the crystal unit cell, the resonances of carbons nearby nitrogen sites can also be split by the through-space dipolar coupling with the quadrupolar nitrogen nucleus.

This type of splitting cannot be removed by magic angle spinning, because the nitrogen quadrupole interaction tilts the quantization axis of nitrogen away from the applied magnetic field. Consequently, the $^{13}C-^{14}N$ dipolar coupling persists, regardless of the sample spinning speed. At a carbon resonance frequency of 50 MHz, this kind of resonance usually appears as an asymmetric doublet. Such doublets have been observed in the NMR spectra of other alkaloids such as morphine (Hexem et al., 1983). The doubling of resonances due to multiple sites in the unit cell have sometimes been mistaken for dipolar coupling (Hollingsworth and Cyr, 1990). In the case of nicotine ditartrate, both types of resonance doubling are observed, as indicated in Table 2. Integration of the spectrum helps to distinguish single carbon resonances. In the aromatic region, the complicated spectral pattern between 145 and 151 ppm corresponding to the C-2, C-4, and C-6 resonances results from a combination of dipolar splitting, multiple sites, and overlapping resonances. The large spread of chemical shifts found in Table 2 for individual carbons in different frozen conformations helps to the explain the absence of resolved nicotine resonances in the tobacco spectra.

Long Contact Time Experiments. At contact times longer than 750 μs, the enhanced ^{13}C polarization begins to decay due to the effect of proton rotating frame relaxation (Yannoni, 1982). In a heterogeneous material such as plant tissue, it is not unusual to observe differential rates of decay for different groups of carbon resonances. This can occur when there is a sufficient number of molecular groups within a homogeneous domain undergoing angular oscillations or rotations at rates that differ significantly from the motion in other domains. Usually, the resonances of molecular groups contained within the same homogeneous domain decay with the same time constant since a process called spin diffusion acts to average out any differences in proton spin polarization within that domain (Yannoni, 1982). The existence of two distinct polysaccharide domains within plant cell walls exhibiting different proton relaxation rates was first demonstrated in bean seedlings by proton wide-line NMR (MacKay et al., 1982, 1988). More recently, differential proton rotating frame relaxation has been observed by ^{13}C CPMAS NMR in tobacco (Wooten, 1991), wood (Newman and Hemmingson, 1990), and other plant materials (Cyr et al., 1990).

The effects of proton rotating frame relaxation can be exploited to simplify the ^{13}C CPMAS NMR spectrum of tobacco and to learn details about tobacco structure. Choosing a contact time long enough to allow the resonances of the most rapidly relaxing components to decay away enhances the relative intensity of the most persistent carbon resonances. These carbons will in general be found in either the most mobile components, such as waxes (e.g. solanesol), or the least mobile components, such as rigid polymers (e.g. cellulose). The ^{13}C CPMAS NMR spectra of the bright and burley tobacco laminae obtained with a 6 ms contact time are shown in Figure 6. These spectra can be compared to the corresponding spectra obtained with a 750 μs contact time found in Figure 2.

With the longer contact time, the resonance pattern in the carbohydrate region has clearly become more cellulose-like. In both the bright and burley tobacco spectra, carbon resonance intensity diminishes at 55, 69, 101, and 176 ppm relative to the cellulose anomeric

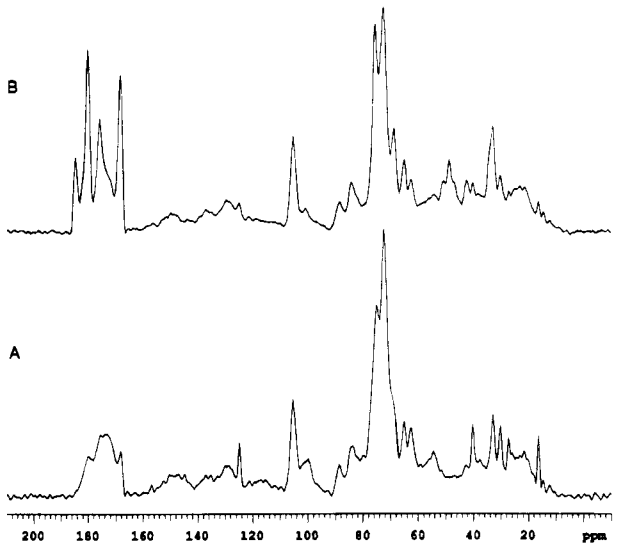

Figure 6. ^{13}C CPMAS NMR spectra of bright (A) and burley (B) tobacco laminae obtained with a 6 ms contact time.

carbon resonance at 105 ppm. All of these resonances correspond to different carbons in pectin (see Figure 4C), a less ordered and more mobile polymer than cellulose. In addition, there is an overall lessening of the broad background resonances in the aliphatic region, suggesting that most of the protein is associated with the pectin, not the cellulose. The intensity of the resonance at 33 ppm changes very little at the longer contact time. This probably is because the predominant type of motion exhibited by the waxy hydrocarbon chains occurs at frequencies that are too high for efficient rotating frame relaxation, and also because the wax occurs mostly on leaf surfaces where it does not mix with the homogeneous domain containing the faster relaxing pectin component. The sharp peaks appearing prominently at 16.4, 30.3, 40.2, and 124.8 ppm in the bright tobacco lamina spectrum (Figure 6A) are due to solanesol, a polyisoprenoid wax (Wooten, 1985). The solanesol carbons, because of their high rotational mobility, will very slowly polarize only if the proton and carbon radio frequency power levels are carefully matched for cross-polarization. Its resonances appear in the spectrum at contact times of 3–5 ms and then persist at contact times longer than 15 ms, due to inefficient proton rotating frame relaxation. Similar cross-polarization behavior has been observed in the triglyceride oils in soybeans by Haw and Maciel (1983). At the opposite extreme of rotational motion, the most rigid components are too immobile to induce efficient rotating frame relaxation. This explains the persistence at the 6 ms contact time of the sharp carboxylate carbon resonances at 180 and 185 ppm of the organic acid salts and of the calcium oxalate resonance at 168.3 ppm.

Calcium Oxalate. Oxalic acid is the end product of several major biochemical pathways. In plants, microscopic calcium oxalate crystals form in specialized plant structures called idioblasts or crystal cells (Franceschi and Horner, 1980; Libert and Franceschi, 1987). If the time domain signal of the tobacco spectrum is Fourier transformed without having the usual apodization function applied, so as to preserve the natural spectral resolution, it can be shown that the resonance at 168 ppm is due to these microcrystals, rather than just amorphous calcium oxalate dispersed within the leaf lamina. Figure 7 shows an expanded spectral region containing the 168 ppm resonance from the bright and burley tobacco lamina spectra processed without any

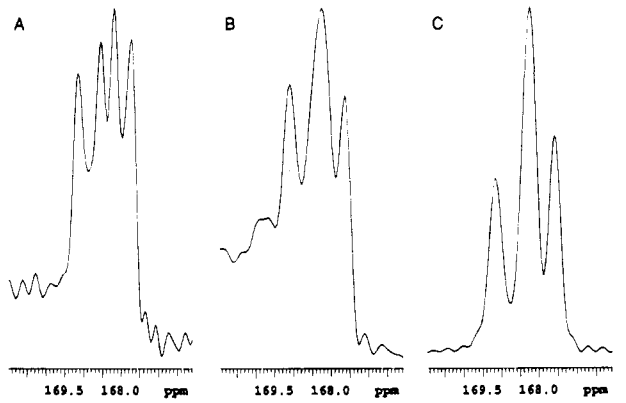

Figure 7. Spectral expansions showing resonances due to calcium oxalate: (A) bright tobacco lamina, (B) burley tobacco lamina, (C) pure calcium oxalate monohydrate (Fisher Scientific).

filter function. Also shown in Figure 7 is a spectrum of pure calcium oxalate monohydrate processed in the same way. The burley tobacco spectrum exhibits a triplet structure with peaks at 167.6, 168.2, and 169.1 ppm, identical to the calcium oxalate spectrum. The multiplicity of peaks can be attributed to a pair of overlapping doublets, corresponding to two pairs of nonequivalent carboxylic acid groups contained in a crystal unit cell containing two nonequivalent molecules of calcium oxalate. In the bright tobacco spectrum, four resonances are actually resolved (167.7, 168.2, 168.5, and 169.1 ppm). The conditions that lead to the splitting of the peak at 168.2 ppm into two resonances are not known, but the history of the particular tobacco sample may influence the uniformity of the calcium oxalate crystals, thereby affecting the resolution. Calcium oxalate crystals in different plant species are commonly observed to have different crystal morphologies (Franceschi and Horner, 1980).

The very sharp resonances (ca. 22 Hz line width) observed for calcium oxalate are characteristic of crystalline organic solids. If there is any amorphous oxalate present in the tobacco, its presumably broader resonance probably adds to the background. The intensity of the calcium oxalate resonances is greater when observed with a 6 ms contact time (Figure 6), as compared to a 750 μs contact time (Figure 2), because, like solanesol, the cross-polarization process is very slow. Unlike solanesol, however, calcium oxalate has a very rigid structure. In this case, the slow cross-polarization occurs because there are no protons directly bonded to the carbons in the oxalate structure to effect cross-polarization. This means that the transfer of spin polarization must come from the protons in the water molecules of hydration in the crystal lattice, a less efficient process since they are remote from the carbon sites. The restricted motion of these water molecules also causes the rotating frame relaxation to be very slow. Thus, the calcium oxalate resonances, like those of solanesol, persist at contact times longer than 15 ms, when all of the remaining tobacco resonances have disappeared.

Dipolar Dephasing Experiments. The dipolar dephasing experiment (Alemany et al., 1983), also known as interrupted decoupling (Opella and Frey, 1979), utilizes a modified cross-polarization pulse sequence that briefly gates the proton decoupler off before data acquisition. During this interval, the strong dipolar interactions between protons and carbon nuclei that are normally removed by continuous, high-power

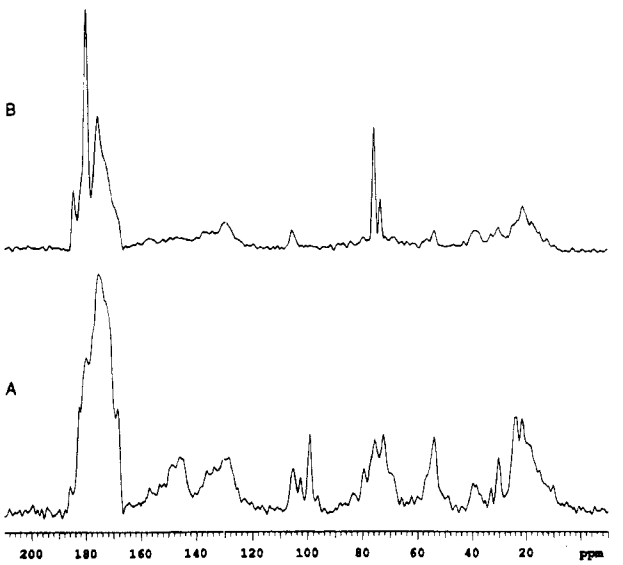

Figure 8. ^{13}C CPMAS NMR spectra of bright (A) and burley (B) tobacco laminae obtained with a 750 μs contact time and a 40 μs decoupler delay (dipolar dephasing).

radio frequency irradiation at the proton resonance frequency cause the carbon spins to lose their phase coherence, thereby attenuating or completely destroying their resonance signals. The resonances that remain are those of carbon nuclei that are only weakly dipolar coupled to protons. These include immobile, nonprotonated carbons, and carbons for which the molecular motions are sufficient to reduce the strength of the dipolar interactions, such as methyl carbons. The dipolar dephasing experiment has been applied to help assign the carbon resonances in the ^{13}C NMR spectra of plants and to reduce the spectral crowding of resonances (Maciel et al., 1985).

The ^{13}C CPMAS NMR spectra of bright and burley tobacco laminae obtained with a 40 μs decoupler delay are shown in Figure 8. Both spectra exhibit a band of methyl resonances centered at ca. 20 ppm. These resonances are due primarily to methyl group side chains in free amino acids and protein, acetyl groups in hemicellulose, methyl groups in rhamnose, rutin, and other materials. The weak resonance at 30 ppm corresponds to polymethylene groups with sufficient segmental mobility to resist complete dephasing. The weak resonance at ca. 38–39 ppm is apparently due to the methyl resonance of nicotine (see Figure 3A). The resonance at 54 ppm corresponds to methoxyl carbons, predominantly due to esterified carboxyl carbons in pectin. The relative intensity of the methoxyl resonance appears to be greater in the bright tobacco spectrum, consistent with the same result in the normal CPMAS spectra. Since the quantities of pectin in bright and burley tobacco are very similar, the greater intensity of the methoxyl resonance in the bright tobacco spectrum suggests that the degree of esterification of the pectin in bright tobacco is higher than in burley tobacco. This result is supported by the increased intensity of the carboxyl resonance at 172 ppm in the bright tobacco spectrum relative to the burley tobacco spectrum, as the pectin ester carbonyl carbons appear at 172 ppm, compared to 175 ppm for free carboxyl group carbons. However, because of the uncertainties associated with the relative rates of cross-polarization in the two samples, this conclusion should be regarded as tentative.

The differences in the carbohydrate region of the dipolar dephased spectra of bright and burley tobacco

laminae reflect the differences in the curing practices of the two types of tobacco. Bright tobacco is flue cured at progressively elevated temperatures. In this curing method, most of the sugars formed in the leaf by the hydrolysis of starch during the early stages of curing are preserved. One of these sugars, fructose, contains a nonprotonated carbon that can be detected by dipolar dephasing. The resonance appearing at 99 ppm in Figure 8A has been assigned to the nonprotonated carbon of fructose (Maciel et al., 1985; Pfeffer, 1983). Burley tobacco, by contrast, is slowly air cured, which allows most of the sugars to be metabolized before the leaf stabilizes. The fructose resonance at 99 ppm is absent in the spectrum of burley tobacco lamina; instead, two sharp peaks corresponding to the quaternary carbon in citric acid salts appear at 73.6 and 76.0 ppm. Citric acid is a byproduct of sugar metabolism. The two resonances may be due to different potassium, calcium, or mixed salts of citric acid (see Table 1). The observations of high levels of fructose in bright tobacco and citrate in burley tobacco are consistent with the amounts of reducing sugars and citrate in bright and burley tobacco reported by Bokelman and Ryan (1985).

In the aromatic region, essentially two broad peaks are observed, centered at ca. 130 and 146 ppm for both bright and burley tobacco laminae. The resonance at 146 ppm is distinctly more intense in the bright tobacco spectrum than in the burley tobacco spectrum. The only nonprotonated aromatic carbon in nicotine is C-3, the resonance of which appears at 133 ppm, so any contribution from nicotine appears in the 130 ppm envelope. The dominant aromatic resonance from aromatic amino acid side chains also appears in the 130 ppm group of peaks. Thus, the enhanced intensity at 146 ppm in the bright tobacco spectrum is probably due to chlorogenic acid and rutin (see Table 2), which are reported at significant levels in bright, but not burley, tobacco. The carboxyl carbon region of both the bright and burley tobacco spectra is composed entirely of resonances of nonprotonated carbons and is essentially unchanged from the same region in the normal CPMAS spectra.

Single-Pulse Experiments. ^{13}C MAS NMR spectra of solid materials are usually obtained with cross-polarization to improve the spectral sensitivity. The pulse repetition rate in the cross-polarization experiment is determined by the spin–lattice relaxation time of the protons, rather than the carbon nuclei. Since proton relaxation times are usually much shorter than carbon relaxation times, a faster pulse repetition rate can be employed. The sensitivity gained by increasing the pulse rate is usually more significant than the enhancement gained from the polarization transfer. In principle, given sufficient time for ^{13}C relaxation, a spectrum equivalent to the CPMAS spectrum can be obtained by using single radio frequency pulses in the same way as for conventional solution NMR. However, if a delay time of just a few seconds is employed, only those carbon nuclei with the shortest relaxation times will be detected. The single-pulse MAS NMR experiment also detects components that do not cross-polarize because they undergo very rapid rotational motion that averages out the proton–carbon dipolar interactions required for cross-polarization, as in the case of liquids.

The single-pulse ^{13}C MAS spectra of bright and burley tobaccos obtained with a 2 s pulse delay are shown in Figure 9. The very sharp, intense resonances in these spectra are due to solanesol, hydrocarbon waxes, and other components that have liquid-like mobility (Wooten, 1985). Because the molecular motion in these components is sufficient to remove most of the resonance broadening due to chemical shift anisotropy and proton–carbon dipolar coupling, magic angle spinning is not essential to observe these resonances. MAS does, however, considerably sharpen the peaks by removing local field inhomogeneities due to variations in magnetic susceptibility within the sample (Wooten, 1985; Ni and Eads, 1992). The broad resonances that appear in the single-pulse spectra are due to carbons with very short ^{13}C relaxation times not saturated by the rapid pulsing. These same broad features do not appear in the previously reported ^{13}C single-pulse MAS spectra of tobacco (Wooten, 1985). The reason is that a much lower proton decoupler power was employed in the prior study; to observe the narrow carbon resonances of the very mobile waxy components, it is only necessary to remove the relatively weak proton–carbon scalar coupling (J coupling). Very high power radio frequency irradiation of the protons ("dipolar decoupling") is required to observe the less mobile carbons, so that the resolution will not be limited by the strong proton–carbon dipolar interactions. The interesting aspect of the broad features is that their resonance profile contains fewer resolved spectral features than in the comparable cross-polarization spectra. The population of carbons represented by the broad resonances must be due to either carbons in close proximity to trace paramagnetic centers such as Mn and Cu (Irwin et al., 1985) or carbons in surface molecular groups that have sufficient rotational mobility at frequencies near 50 MHz to permit rapid relaxation.

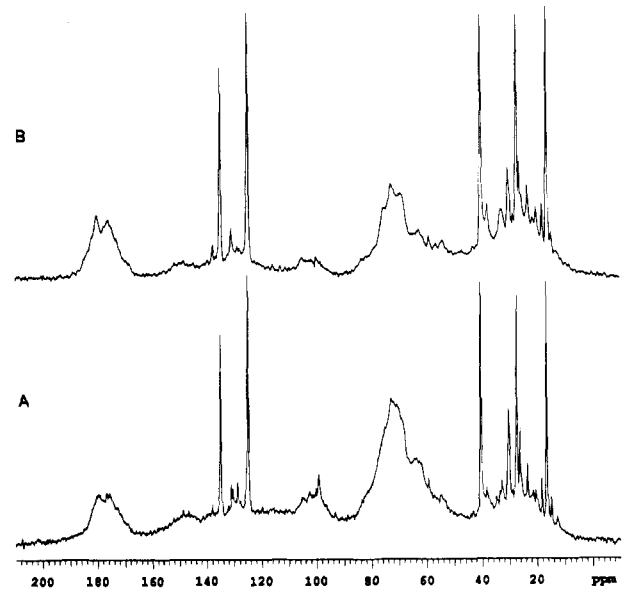

Figure 9. ^{13}C single-pulse MAS NMR spectra obtained with high-power (dipolar) decoupling of bright (A) and burley (B) tobacco laminae.

Stems. The ^{13}C CPMAS spectra of bright and burley tobacco stems obtained with a 750 μs contact time are shown in Figure 10. The cellulose content of both bright and burley tobacco stems is at least twice that of the lamina, while the amount of either pectin or hemicellulose in the stems is roughly the same as in the lamina. The greater amount of cellulose is reflected by the enhanced prominence of the cellulose carbon resonances in the stem spectra in comparison to the spectra of the laminae. The difference between the spectra of bright and burley tobacco stems is small; primarily, the overall resonance intensity in the carbohydrate and carboxyl regions is greater in the bright tobacco stem spectrum.

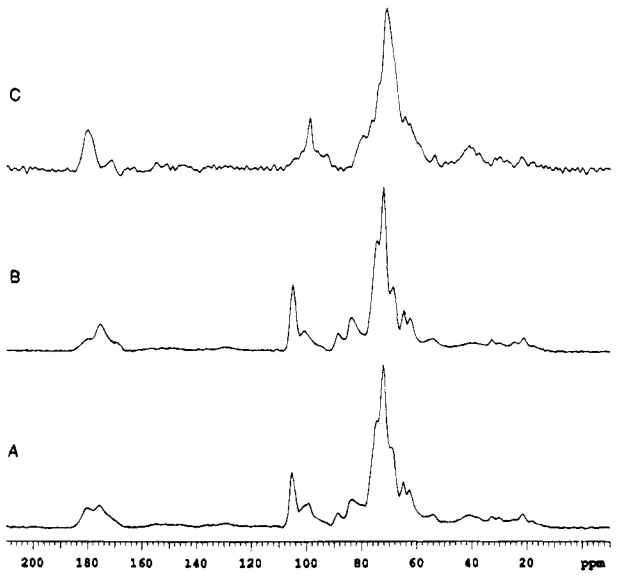

Figure 10. ^{13}C CPMAS NMR spectra of bright (A) and burley (B) tobacco stems obtained with a 750 μs contact time. Spectrum C is the difference between spectra A and B.

The differences in resonance intensity between bright and burley tobacco are easier to distinguish by subtracting the two spectra. This difference spectrum is shown in Figure 10C. There are weak resonances in the difference spectrum at ca. 40 and 180 ppm. These resonances reflect the higher content of malate (7.8%) in bright tobacco stems in comparison to burley tobacco stems (4.8%). The resonances in the carbohydrate region reflect the high level of reducing sugars found in bright tobacco stems (12.9%) but are absent in the burley tobacco stems. The malate C–OH resonance also appears in the same region at ca. 68 ppm. As noted earlier, the resonance appearing at 99 ppm is attributed to the anomeric carbon of fructose.

DISCUSSION

Considering the complexity of the chemical composition of tobacco, a surprising number of components can be distinguished in the ^{13}C NMR spectra of the intact plant tissue, even though only a few components can be detected without some obfuscation due to background and coincident resonances. The components that can be observed with the least interference include cellulose (detected via its C-4 resonance at 89 ppm), calcium oxalate (detected via its resonance at 168.2 ppm by long contact time cross-polarization), citrate salts and fructose (detected via their quaternary carbons by dipolar dephasing), nicotine (detected via its methyl group resonance by dipolar dephasing), and solanesol and hydrocarbon wax (detected by single-pulse excitation). The observation of other components is limited to classes such as organic acids (via their carboxyl carbons), phenolics (via the aromatic resonances at ca. 150 ppm and by dipolar dephasing), and non-cellulose polysaccharides (via anomeric carbon resonances at 101–103 ppm). The analysis of the polysaccharides by NMR is particularly valuable since the process of isolating these components by chemical methods is difficult. Fortunately, the carbohydrate region is relatively easy to interpret as a composite spectrum of cellulose, hemicellulose, and pectin. This analysis can be improved if the tobacco samples are washed with water to remove the soluble organic acids and monosaccharides, which have interfering resonances in the same region.

Table 3. Cross-Polarization Parameters for Selected Resonances of Bright Tobacco

ppm	M_0	T_{CH} (μs)	$T_{1\rho}$ (μs)	M/M_0[a]	$(M/M_0)_c$[b]
22.5	62.9	80.7	4126	0.85	0.98
25.4	65.4	58.3	3858	0.84	0.96
30.7	69.3	64.5	4172	0.85	0.98
33.3	79.2	45.3	4418	0.85	0.98
39.9	71.7	50.5	3180	0.80	0.92
54.6	78.5	60.6	3250	0.81	0.93
63.5	126.6	38.1	2899	0.78	0.90
65.5	139.6	38.5	2919	0.78	0.90
69.6	265.7	45.2	2515	0.76	0.87
72.8	475.0	53.5	3332	0.81	0.93
75.4	276.7	51.8	3517	0.82	0.94
84.5	78.1	49.8	3708	0.83	0.95
88.0	30.4	34.6	6494	0.90	1.03
100.4	83.8	80.5	2852	0.79	0.91
105.6	100.0	66.0	4930	0.87	1.00
116.6	18.2	38.3	5246	0.87	1.00
129.6	33.0	190.1	6229	0.90	1.03
148.9	20.6	169.9	8571	0.92	1.06
175.7	109.1	408.4	4479	0.78	0.90
179.9	83.1	432.2	4593	0.77	0.89

[a] Computed from the relation $M/M_0 = [1/(1 - T_{CH}/T_{1\rho})](e^{-\tau/T_{1\rho}})(1 - e^{-\tau/T_{CH}})$ for a contact time of τ = 750 μs and the experimental values of M_0, T_{CH}, and $T_{1\rho}$. [b] $(M/M_0)_c$ is the value of M/M_0 relative to the value for the cellulose resonance at 105.5 ppm $[(M/M_0)/0.87]$.

In the application of NMR spectroscopy to the characterization of tobacco and other plants, quantitative comparisons are likely to be important. Quantitative measurements by ^{13}C CPMAS NMR, however, are complicated by the complexity of the spectra and the vagaries of the cross-polarization experiment. Nonetheless, by taking appropriate experimental precautions, and by employing appropriate analytical strategies, good quantitative results can be obtained. When resonance intensities are compared, the most important consideration is to ensure that individual carbon resonances cross-polarize with similar efficiency. Two examples can be cited which exemplify the difficulties involved. In spectra obtained with a 750 μs contact time, the calcium oxalate resonance at 168 ppm cannot be compared quantitatively with any of the other resonances. Its polarization transfer time (T_{CH}) is much too long, and it does not reach full polarization until much longer contact times. By a similar token, in spectra obtained with contact times longer than ca. 2 ms, the anomeric carbon resonance of pectin at 103 ppm is not comparable to the cellulose resonance at 105 ppm. Its proton rotating frame relaxation time (^1H $T_{1\rho}$) is shorter than for cellulose, and its resonance diminishes more quickly. Fortunately, at 750 μs nearly full ^{13}C polarization is obtained for most resonances before significant rotating frame relaxation occurs.

An accurate determination of cross-polarization intensities requires a knowledge of T_{CH} and ^1H $T_{1\rho}$ for each carbon site. Values for these rate constants can be obtained by measuring the resonance intensities as a function of contact time (Schaefer and Stejskal, 1979). For a complex material such as tobacco, multiple contact time experiments can be time-consuming, because long acquisition times may be needed to observe some of the weak spectral features. Nonetheless, it is worthwhile to perform such experiments on some samples to determine the degree of uncertainty associated with single contact time experiments. Tables 3 and 4 show the results of multiple contact time experiments for selected resonances of bright and burley tobaccos, respectively. The quantity M_0 represents the expected resonance intensity if the value of T_{CH} were infinitely

Table 4. Cross-Polarization Parameters for Selected Resonances of Burley Tobacco

ppm	M_0	T_{CH} (μs)	$T_{1\rho}$ (μs)	M/M_0[a]	$(M/M_0)_c$[b]
21.8	77.6	76.4	4129	0.85	0.97
25.1	82.8	52.6	3923	0.84	0.96
30.6	87.3	51.9	3804	0.83	0.95
33.2	109.4	48.9	5122	0.87	1.00
38.4	81.6	44.8	3283	0.81	0.92
40.5	78.7	40.6	3569	0.82	0.94
48.7	83.1	32.9	4727	0.86	0.98
54.4	76.1	50.4	3642	0.83	0.94
63.0	91.0	36.1	3999	0.84	0.95
65.4	108.2	33.0	4172	0.84	0.96
69.5	290.0	48.0	3281	0.81	0.92
72.7	392.0	60.9	4096	0.85	0.96
75.5	285.1	74.5	4428	0.86	0.98
83.6	71.2	49.8	4219	0.85	0.97
88.8	27.1	39.7	6210	0.89	1.02
101.9	55.4	44.4	3335	0.81	0.92
105.5	100.0	67.5	5158	0.88	1.00
130.1	47.1	265.6	3432	0.82	0.94
137.4	19.2	137.2	5153	0.88	1.01
149.2	21.3	47.3	4856	0.87	0.99
168.8	50.4	653.6	44906	0.68	0.78
175.9	151.2	355.8	5264	0.82	0.93
180.2	253.3	532.6	4728	0.73	0.83

[a] Computed from the relation $M/M_0 = [1/(1 - T_{CH}/T_{1\rho})](e^{-\tau/T_{1\rho}})(1 - e^{-\tau/T_{CH}})$ for a contact time of $\tau = 750$ μs and the experimental values of M_0, T_{CH}, and $T_{1\rho}$. [b] $(M/M_0)_c$ is the value of M/M_0 relative to the value for the cellulose resonance at 105.5 ppm $[(M/M_0)/0.88]$.

short and $T_{1\rho}$ infinitely long. Since many comparisons were made between resonances within and between spectra obtained with a 750 μs contact time, it is valuable to compare the resonances intensities (M) that would be expected at 750 μs relative to full polarization (M_0). On the basis of experimentally determined values of M_0, T_{CH}, and $T_{1\rho}$, theoretical values of M/M_0 were computed. The results given in Tables 3 and 4 show that most carbons reach 80–90% of full polarization at 750 μs.

A more useful basis for comparison is the intensity of one resonance peak relative to another obtained at the same contact time (Irwin et al., 1985). As indicated earlier, the cellulose anomeric carbon resonance at 105.5 ppm is convenient for this purpose. The values of M/M_0 normalized to the respective values for cellulose in bright and burley tobacco laminae are also given in Tables 3 and 4. These ratios show that the resonance intensities for nearly all of the resonances, with a few exceptions such as some of the carboxyl carbons, are within 10% of their expected values. These results validate the comparisons made on the basis of single contact time experiments of the current samples, but they are not necessarily transferable to samples that have been processed or cured under different conditions. In particular, it should be expected that samples conditioned at higher moisture levels may have T_{CH} and $T_{1\rho}$ values that differ from those presented here. Further issues relating to quantitative measurements by ^{13}C CPMAS NMR have been addressed in more detail elsewhere (Schaefer and Stejskal, 1979; Irwin et al., 1985; Irwin, 1989; Hatfield et al., 1987; Maciel et al., 1985).

The overlap of resonance lines also presents a significant obstacle toward quantitative measurements, but various schemes to overcome this problem have been reported. In some cases, the extent of overlap can be estimated on the basis of the expected composition of the sample. This approach has most successfully been applied to wood, for which reasonable estimates of the overlap between lignin and polysaccharide resonances can be made (Haw et al., 1984; Bates and Hatcher, 1992). Another successful method has been to compare an unknown plant sample to a set of samples with known composition and to utilize the multivariate calibration technique called partial least squares (Wallbacks et al., 1991). This approach has been used in our laboratory to estimate the amount of stems in tobacco blends. Sometimes a complete or partial deconvolution of the spectrum can be accomplished. One way to do this is by curve fitting, if the number of components is known. In some favorable cases, spectral editing experiments can sometimes be performed on the basis of the differences between individual components in NMR rate phenomenon, for example, rotating frame relaxation (Newman and Hemmingson, 1990; Cyr et al., 1990; Wooten, 1991). Recently developed spectral editing experiments hold promise for providing subspectra of methylene and methine carbons, as well as for nonprotonated and methyl carbons (Wu and Zilm, 1993; Wu et al., 1994). The application of these cross-polarization pulse sequences, however, may be limited to the most intense resonances, because they rely on the use of a short contact time (40 μs), which significantly reduces the spectral sensitivity.

The tobacco samples used in this study were blended, commercial samples of indeterminate origin. Their ^{13}C NMR spectra consequently reflect an average tobacco composition. The results presented in this paper, however, demonstrate that ^{13}C CPMAS NMR should be capable of providing rapid analysis of individual cultivars and different plant structures. Both the bright and burley tobacco samples employed were cured according to their traditional methods. From the standpoint of NMR analysis, this turns out to be fortuitous, since green tobacco contains as much as 43% starch by dry weight. The curing process dramatically reduces the amount of starch in the leaf lamina (Ryan et al., 1985). Thus, the carbohydrate region in the spectra of the cured tobacco samples is not overwhelmed by starch resonances. Although green tobacco has not been investigated by ^{13}C NMR, it can be expected that the large amount of starch in the lamina will significantly obscure some of the spectral features that stand out in the spectra of the cured samples.

ACKNOWLEDGMENT

I am indebted to Gordon Bokelman, Bill Ryan, John Paine, and Richard Izac for providing samples and for helpful discussions.

LITERATURE CITED

Alemany, L. B.; Grant, D. M.; Alger, T. D.; Pugmire, R. J. Cross polarization and magic angle sample spinning NMR spectra of model organic compounds 3. Effect of the ^{13}C-H dipolar interaction on cross polarization and carbon-proton dephasing. *J. Am. Chem. Soc.* **1983**, *105*, 6697.

Baianu, I. C. High-resolution NMR studies of food proteins. In *Nuclear Magnetic Resonance in Agriculture*; Pfeffer, P. E., Gerasimowicz, W. V., Eds.; CRC Press: Boca Raton, FL, 1989; Chapter 6.

Bates, A. L.; Hatcher, P. G. Quantitative solid-state ^{13}C nuclear magnetic resonance spectrometric analyses of wood xylem; effect of increasing carbohydrate content. *Org. Geochem.* **1992**, *18*, 407.

Bokelman, G. H.; Ryan, W. S., Jr. Analyses of bright and burley tobacco laminae and stems. *Beitr. Tabakforsch. Int.* **1985**, *13*, 29.

Bokelman, G. H.; Ryan, W. S., Jr.; Oakley, E. T. Fractionation of bright tobacco. *J. Agric. Food Chem.* **1983**, *31*, 897.

Cyr, N.; Elofson, R. M.; Mathison, G. W. Determination of crystallinity of carbohydrates by ^{13}C cross polarization/magic

angle spinning NMR with applications to the nutritive value of forages. *Can. J. Anim. Sci.* **1990**, *70*, 695.
Elofson, R. M.; Ripmeester, J. A.; Cyr, N.; Milligan, L. P.; Mathison, G. W. Nutritional evaluation of forages by high resolution solid state ^{13}C NMR. *Can. J. Anim. Sci.* **1984**, *64*, 93.
Franceschi, V. R.; Horner, H. T., Jr. Calcium oxalate crystals in plants. *Bot. Rev.* **1980**, *46*, 361.
Garleb, K. A.; Bourquin, L. D.; Hsu, J. T.; Wagner, G. W.; Schmidt, S. J.; Fahey, G. C. Isolation and chemical analyses of nonfermented fiber fractions of oat hulls and cotton-seed hulls. *J. Anim. Sci.* **1990**, *69*, 1255.
Hatfield, G. R.; Maciel, G. E.; Erbatur, O.; Erbatur, G. Qualitative and quantitative analysis of solid lignin samples by carbon-13 nuclear magnetic resonance spectrometry. *Anal. Chem.* **1987**, *59*, 172.
Haw, J. F. Solid-state NMR studies of treated wood and lignin. In *Nuclear Magnetic Resonance in Agriculture*; Pfeffer, P. E., Gerasimowicz, W. V., Eds.; CRC Press: Boca Raton, FL, 1989; Chapter 12.
Haw, J. F.; Maciel, G. E. Carbon-13 nuclear magnetic resonance spectrometry of oil seeds with cross polarization and magic-angle spinning. *Anal. Chem.* **1983**, *55*, 1262.
Haw, J. F.; Maciel, G. E.; Schroeder, H. A. Carbon-13 nuclear magnetic resonance spectrometric study of wood and wood pulping with cross polarization and magic-angle spinning. *Anal. Chem.* **1984**, *56*, 1323.
Hexem, J. G.; Frey, M. H.; Opella, S. J. ^{13}C NMR of crystalline morphine. *J. Am. Chem. Soc.* **1983**, *105*, 5717.
Himmelsbach, D.; Barton, F. E.; Windham, W. R. Comparison of carbohydrate, lignin, and protein ratios between grass species by cross polarization-magic angle spinning carbon-13 nuclear magnetic resonance. *J. Agric. Food Chem.* **1983**, *31*, 401.
Hollingsworth, M. D.; Cyr, N. High resolution solid-state NMR spectra of leucine: a re-examination. *J. Chem. Soc., Chem. Commun.* **1990**, 578.
Irwin, P. L. The structure and degradation of intact plant cell wall matrices by ^{13}C CPMAS NMR and related techniques. In *Nuclear Magnetic Resonance in Agriculture*; Pfeffer, P. E., Gerasimowicz, W. V., Eds.; CRC Press: Boca Raton, FL, 1989; Chapter 11.
Irwin, P. L.; Pfeffer, P. E.; Gerasimowicz, W. V.; Pressey, R.; Sams, C. E. Ripening-related perturbations in apple cell wall nuclear spin dynamics. *Phytochemistry* **1984**, *23*, 2239.
Irwin, P. L.; Gerasimowicz, W. V.; Pfeffer, P. E.; Fishman, M. ^{1}H-^{13}C polarization transfer studies of uronic acid polymer systems. *J. Agric. Food Chem.* **1985**, *33*, 1197.
Jarvis, M. C. Solid state ^{13}C-NMR spectra of vigna primary cell walls and their polysaccharide components. *Carbohydr. Res.* **1990**, *201*, 327.
Jarvis, M. C.; Apperley, D. C. Direct observation of cell wall structure in living plant tissues by solid-state ^{13}C NMR spectroscopy. *Plant Physiol.* **1990**, *92*, 61.
Kolodziejski, W.; Frye, J. S.; Maciel, G. E. Carbon-13 nuclear magnetic resonance spectrometry with cross polarization and magic-angle spinning for analysis of lodgepole pine wood. *Anal. Chem.* **1982**, *54*, 1419.
Lewis, N. G.; Yamamoto, E.; Wooten, J. B.; Just, G.; Ohashi, H.; Towers, G. H. N. Monitoring biosynthesis of wheat cell-wall phenyl propanoids in situ. *Science* **1987**, *237*, 1344.
Libert, B.; Franceschi, V. R. Oxalate in crop plants. *J. Agric. Food Chem.* **1987**, *35*, 926.
Maciel, G. E.; Haw, J. F.; Smith, D. H.; Gabrielsen, B. C.; Hatfield, G. R. Carbon-13 nuclear magnetic resonance of herbaceous plants and their components, using cross polarization and magic-angle spinning. *J. Agric. Food Chem.* **1985**, *33*, 185.
MacKay, A. L.; Bloom, M.; Tepfer, M.; Taylor, I. E. P. Broadline proton magnetic resonance study of cellulose, pectin, and bean cell walls. *Biopolymers* **1982**, *21*, 1521.
Mackay, A. L.; Wallace, J. C.; Sasaki, K.; Taylor, I. E. P. Investigation of the physical structure of primary plant cell wall by proton magnetic resonance. *Biochemistry* **1988**, *27*, 1467.
Newman, R. H.; Hemmingson, J. A. Determination of the degree of cellulose crystallinity in wood by carbon-13 nuclear magnetic resonance spectroscopy. *Holzforschung* **1990**, *44*, 1990.
Ni, Q. W.; Eads, T. Low speed magic-angle-spinning carbon-13 NMR of fruit tissue. *J. Agric. Food Chem.* **1992**, *40*, 1507.
O'Donnell, D. J.; Ackerman, J. J. H.; Maciel, G. E. Comparative study of whole seed protein and starch content via cross polarization-magic angle spinning nuclear magnetic resonance spectroscopy. *J. Agric. Food Chem.* **1981**, *29*, 514.
Opella, S. J.; Frey, M. H. Selection of nonprotonated carbon resonances in solid-state nuclear magnetic resonance. *J. Am. Chem. Soc.* **1979**, *101*, 5854.
Pfeffer, P. E.; Hicks, K. B.; Earl, W. L. Solid-state structures of keto-disaccharides as probed by ^{13}C cross-polarization, magic-angle spinning NMR spectroscopy. *Carbohydr. Res.* **1983**, *111*, 181.
Pitner, T. P.; Seeman, J. I.; Whidby, J. F. Assignment and solvent dependence of the carbon-13 nuclear magnetic resonance spectrum of nicotine. *J. Heterocycl. Chem.* **1978**, *15*, 1978.
Ryan, W. S., Jr.; Bokelman, G. H.; Sun, H. H.; Terrill, T. R. Influence of genetic and cultural factors on chemical and physical properties of tobacco. *Beitr. Tabakforsch. Int.* **1985**, *13*, 88.
Schaefer, J.; Stejskal, E. O. High resolution C-13 NMR of solid polymers. In *Topics in Carbon-13 NMR Spectroscopy*; Levy, G. C., Ed.; Wiley: New York, 1979; Vol. 3.
Slaven, R. W. The carbon-13 and proton NMR spectra of nicotine in aqueous media. *J. Heterocycl. Chem.* **1984**, *21*, 1329.
Sun, H. H.; Wooten, J. B.; Ryan, W. S., Jr.; Bokelman, G. H.; Aman, P. Structural characterization of a tobacco rhamnogalacturonan. *Carbohydr. Polym.* **1987**, *7*, 143.
VanderHart, D. L.; Atalla, R. H. Studies of microstructure in native celluloses using solid-state ^{13}C NMR. *Macromolecules* **1984**, *17*, 1465.
Wallbacks, L.; Edlund, U.; Norden, B.; Berglund, I. Multivariate characterization of pulp using solid-state ^{13}C NMR, FTIR, and NIR. *Tappi J.* **1991**, Oct, 201.
Westerlund, E.; Aaman, P.; Andersson, R. E.; Andersson, R. Investigation of the distribution of methyl ester groups in pectin by high-field carbon-13 NMR. *Carbohydr. Polym.* **1990**, *14*, 179.
Wooten, J. B. Direct detection of solanesol in tobacco by ^{1}H and ^{13}C magic angle spinning NMR. *J. Agric. Food Chem.* **1985**, *33*, 419.
Wooten, J. B. Rotating frame relaxation effects in the ^{13}C CPMAS NMR spectra of tobacco. *Abstracts of Papers*, The 45th Tobacco Chemists' Research Conference, Ashville, NC, Oct 20, 1991.
Wu, X.; Zilm, K. W. Methylene-only susbspectrum in CPMAS NMR. *J. Magn. Reson., Ser. A* **1993**, *104*, 119.
Wu, X.; Burns, S. T.; Zilm, K. W. Spectral editing in CPMAS NMR. Generating subspectra based on proton multiplicities. *J. Magn. Reson., Ser. A* **1994**, *111*, 29.
Wuthrich, K. *NMR in Biological Research: Peptides and Proteins*; American Elsevier: New York, 1976; p 175.
Wynder, E. L.; Hoffmann, D. *Tobacco and Tobacco Smoke*; Academic Press: New York, 1967; pp 41–42.
Yannoni, C. S. High-resolution NMR in solids: the CPMAS experiment. *Acc. Chem. Res.* **1982**, *15*, 201.
Yosef, E.; Ben-Ghedalia, D.; Miron, J.; Huttermann, A.; Majcherczyk, A.; Milstein, O.; Ludemann, H. D.; Frund, R. Characterization of some cell wall components of untreated and ozone-treated cotton stalks. *J. Agric. Food Chem.* **1994**, *42*, 86.

Received for review February 7, 1995. Revised manuscript received July 26, 1995. Accepted September 15, 1995.[⊗]

JF950082O

[⊗] Abstract published in *Advance ACS Abstracts,* November 1, 1995.